Observation of Standing Acoustic Waves by Resonant Raman Scattering

A. Mlayah,[1] R. Grac,[1] G. Armelles,[2] R. Carles,[1] A. Zwick,[1] and F. Briones[2]
[1]*Laboratoire de Physique des Solides, ERS/CNRS 5646, Université Paul Sabatier, 118 route de Narbonne, 31062 Toulouse Cedex, France*
[2]*Instituto de Microelectronica de Madrid, Consejo Superior de Investigaciones Cientificas, Isaac Newton 8, Parque Tecnologico de Madrid, E-28760 Tres Cantos Madrid, Spain*
(Received 19 February 1997)

Resonant Raman measurements on GaAs/GaP quantum wells, as thin as one monolayer, are reported. The work is focused on the low-frequency scattering range, which exhibits a continuous emission and periodic oscillations that have never been observed up to now. It is shown that spatial localization of electrons leads to Raman scattering processes for which momentum is not conserved, and hence to the activation of the density of states of acoustic phonons. A model, based on electron-acoustic phonon interaction, is developed and used for calculations of the resonant Raman efficiency. A good agreement with measured spectra is obtained. The origin of the observed periodic oscillations is interpreted by considering standing acoustic waves. [S0031-9007(97)03207-9]

PACS numbers: 78.30.Fs, 63.20.Dj, 78.66.Fd

During the last decade considerable interest has been devoted to the vibrational properties of semiconductor superlattices (SL's) and multiple quantum wells (QW's), leading to a detailed understanding of phonons and their coupling with electrons [1,2]. It is now well established that, in these structures, vibrational excitations could be confined [3–5] (optical phonons), localized [6,7] (interface phonons), or folded [8] (acoustic phonons) depending on the energy range and on the elastic and dielectric properties of the constituents. Almost all of these features were pointed out by means of Raman scattering measurements. In contrast, only a few results [9,10] are available for single QW's (or even for a small number of QW's), because the associated scattering volume is considerably reduced, leading to a serious experimental limitation. Beyond the experimental challenge, the study of such structures is of particular interest with regard to both vibrational and electronic properties.

Indeed, in single quantum wells electrons are localized in real space which leads to a breakdown of the translational symmetry along the growth axis. In the acoustic frequency range this effect results in a strongly resonant continuous scattering [11,12]. In a previous work [10], we showed that frequency location, line shape, and intensity of the continuous scattering is mainly determined by the form factor associated with localized electron-acoustic phonon interaction. In this Letter, we report on resonant Raman measurements on GaAs/GaP quantum wells as thin as one monolayer. In this extreme situation of electron localization, a strong continuous emission appears again in the low-frequency range. In addition, periodic oscillations of the continuous scattering are observed. The origin of the continuous scattering and its oscillatory behavior is discussed and analyzed by taking into account both spatial localization of electrons and possible existence of standing acoustic waves. A model based on electron-acoustic phonon interaction in a single quantum well is developed, and a comparison between calculated and measured Raman spectra is presented. Our most exciting findings are as follows: (i) electronic wave functions can be obtained from low-frequency resonant Raman spectra; (ii) for the first time, standing acoustic waves could be observed.

The structures investigated were grown by atomic layer molecular beam epitaxy (ALMBE) on a (001) oriented GaP substrate. The samples consist of three GaAs QW's separated by wide (38 nm) GaP barriers. The first QW is at 80 nm underneath the sample surface. The GaAs QW's are of equal thickness ranging from 1 to 4 monolayers (ML) in steps of 1 ML. Only the results obtained from 1 ML GaAs QW's are presented here, since the other samples showed very similar features. The lattice mismatch between GaAs and GaP is about 4% (with respect to GaP), and the critical thickness for dislocation formation (and strain relaxation) is around 6 ML [13]. So, the GaAs QW's are biaxially strained and fully matched to GaP. As a matter of fact, the high energy electron diffraction patterns showed neither three-dimensional growth nor appreciable roughness.

Calculation of the band structure of GaAs strained to GaP was performed according to the deformation potential theory [14]. It was found that the GaAs layer is indirect in k space. Indeed, due to strain, the lowest energy conduction states are of X_{xy} type. For Γ-band electrons, the GaAs layer forms a well which is 0.5 eV deep. The energy of transition between confined heavy hole (hh) and Γ-electron states was determined by electroreflectance spectroscopy performed at liquid nitrogen temperature. It was found at 2.73 eV, for the 1 ML GaAs QW's.

Raman experiments were performed at liquid nitrogen temperature and in near-backscattering configuration. The spectra were excited using the output lines of an Ar laser. The scattered light was analyzed using a triple spectrometer and detected with a conventional photon

0031-9007/97/78(21)/4119(4)$10.00 © 1997 The American Physical Society

counting system. For off-resonance exciting energies, only optical phonons from the GaP layers were observed; it was not possible to detect the Raman signal from the GaAs QW's because of their relatively small scattering volume. In order to overcome this difficulty, resonant exciting energies were used and accumulation times as large as 10 h were needed.

Figure 1(a) presents both Stokes and anti-Stokes regions of the Raman spectrum recorded with exciting energy (2.727 eV) in resonance with the Γ-hh transition of the GaAs QW's. The same spectrum, corrected for Bose-Einstein population factor, is shown in Fig. 1(b).

In the frequency range (270–300 cm^{-1}) of GaAs optical phonons, two lines are clearly observed at 280 and 289 cm^{-1}. The GaAs QW's are only one monolayer thick, and hence only one confined longitudinal optical (LO) mode is expected. By assuming that phonon confinement can be still described by the alternating linear chain model (LCM) [1,2] in such narrow QW's, the LO phonon frequency of a strain-free GaAs monolayer is estimated at 282 cm^{-1}. In fact, the GaAs QW's are matched to GaP and thus submitted to a compressive biaxial strain. As a consequence, confined LO phonons are shifted towards higher frequencies, leading to the line observed at 289 cm^{-1}. The line at 280 cm^{-1} could be due to confined TO (transverse optical) phonons (of a strained GaAs monolayer) activated by deviations from the true backscattering configuration. In order to ascertain the origin of this line, more detailed calculations, out of the scope of this work, are needed since the validity of the LCM becomes questionable for such ultrathin QW's. Nevertheless, the fact that we do observe optical phonons from the GaAs QW's is a direct proof of the resonance condition.

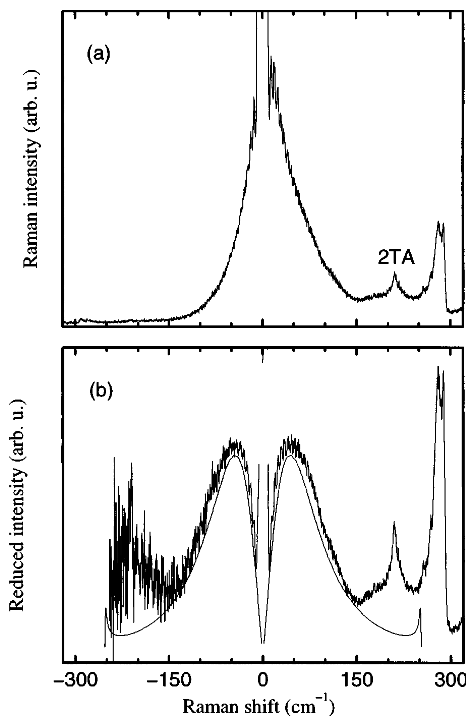

FIG. 1. (a) Raman spectrum recorded in both Stokes and anti-Stokes regions with exciting energy (2.727 eV) in resonance with the Γ-hh transition of the GaAs QW's. (b) Spectrum of (a) after correction for Bose-Einstein population factor. The effective temperature was 100 K. The structure labeled 2TA is due to second-order Raman scattering by transverse acoustic phonons of GaP. The thin line shows the results of calculations.

Now, focusing on the low-frequency range of the spectrum, one notes [Fig. 1(a)] a very strong continuous scattering centered around the excitation line. This scattering appears only under resonant excitation of the GaAs QW's, like for optical phonons. After correcting such spectrum for the Bose-Einstein population factor [Fig. 1(b)], the continuous emission appears as a broad and intense band located around 50 cm^{-1}. In addition, superimposed on this band, periodic oscillations are clearly observed in both Stokes and anti-Stokes regions of the spectrum. The observation of such oscillations in the Raman spectra is reported here for the first time. In what follows, we show that the spatial localization of electrons, and their interaction with standing acoustic phonon waves, are at the origin of the observed continuous emission and its oscillatory behavior.

Let us consider the interaction of confined electrons with longitudinal acoustic (LA) phonons via deformation-potential mechanism. In a first step, propagating LA waves are assumed, which means that the possible existence of standing acoustic waves is ignored. Moreover, in a one monolayer GaAs QW, the electron wave function strongly extends into the GaP barriers, and the probability of finding the electron outside the QW is much higher than inside. Hence, the contribution of the GaAs layers to the electron-phonon interaction is here neglected, and only the interaction of confined electrons with LA phonons of the GaP layers is considered. The electron-phonon interaction Hamiltonian reads [15]

$$H_q = \left(\frac{\hbar a^3}{2M \omega_q V} \right)^{1/2} iqDe^{iqr} a_q + \text{c.c.}, \qquad (1)$$

where D is a deformation-potential constant, a^3 and M are the volume and mass of the primitive cell, respectively, and V is the sample volume; a_q is the phonon creation operator. ω_q and q are, respectively, the frequency and three-dimensional wave vector of bulklike LA phonons.

From Eq. (1) and for intrasubband electron scattering, the Raman efficiency for Stokes and anti-Stokes resonant processes is found proportional to

$$S = \sum_{q_z} (N_{q_z} \mp \tfrac{1}{2} + \tfrac{1}{2}) \frac{q_z^2}{\omega_{q_z}} |M_{q_z}|^2 \times \delta(\hbar\omega_s - \hbar\omega_i \pm \hbar\omega_{q_z}) |(\hbar\omega_s - \hbar\omega_{ex} \pm i\gamma_{ex}) \times (\hbar\omega_i - \hbar\omega_{ex} \pm i\gamma_{ex})|^{-2}, \qquad (2)$$

where N_{q_z} is the Bose-Einstein population factor, q_z is the phonon wave vector along the growth axis (z); $\hbar\omega_e = 2.73$ eV and $\gamma_e \sim 25$ meV are, respectively, the energy and natural linewidth of the Γ-hh transition as estimated from electroreflectance data; $\hbar\omega_i$ and $\hbar\omega_s$ are the incident

and scattered photon energies, respectively. M_{q_z} is a form factor given by the overlap integral

$$M_{q_z} = \int e^{iq_z z} |\varphi(z)|^2 \, dz \,, \qquad (3)$$

in which $\varphi(z)$ is the confined electron wave function. In Eq. (2) translational invariance in the QW's plane is assumed. As a consequence, the in-plane component of the wave vector exchanged (q_{ex}) during the Raman process is zero (in backscattering configuration). In return, this wave vector conservation law is not fulfilled in the z direction because of the spatial localization of electrons. Indeed, for completely delocalized electrons the associated wave function is a plane wave, and thus M_{q_z} is reduced to a delta function. This means that wave vector conservation law is recovered. In this case, only scattering by acoustic phonons, with $q_z = q_{ex}$, is allowed. This is one of the main points of this work, as it clearly appears that spatial localization of electrons allows q_z modes from the whole Brillouin zone to participate in the light scattering. Moreover, from Eq. (2) one notes that the Raman spectrum is mainly determined by the form factor M_{q_z}, which is the Fourier transform of the probability density $|\varphi(z)|^2$. Therefore, the probability density associated with localized electrons can be deduced from the Raman spectrum.

Figure 1(b) presents a comparison between measured and calculated Raman spectra according to Eq. (2). The dispersion relation ω_{q_z} along the (001) direction (confinement direction) of LA phonons in GaP was obtained from a least-square fit to the neutron data [16]. In that way, deviations from the linear dispersion approximation are taken into account. As the GaP barriers are sufficiently wide (38 nm), coupling between GaAs QW's is neglected. For a one monolayer thick QW the spatial variation of the confinement potential can be approximated by a delta function. In this case the eigen-wave function of the confined state decays exponentially from the center of the QW. Thus, we choose $\varphi(z) = a^{-1/2} e^{-|z|/a}$ as a trial function. The calculated Raman spectrum, shown in Fig. 1(b), was obtained with $a = 1$ nm. As it can be seen, the present model accounts well for the observed continuous emission. As a matter of fact, only one monolayer variation in a leads to a peak position shift of 15 cm^{-1}, which underlies the sensitivity of low-frequency Raman scattering to the electronic wave function localization. Moreover, one notes from Eq. (2) that the continuous emission is doubly resonant as far as the energy of LA phonons remains small in comparison with the natural width of the electronic transition [denominators in Eq. (2)]. This double resonance effect explains the strong intensity of the low-frequency scattering (Fig. 1).

Let us come now to the origin of the observed periodic oscillations. As mentioned above, possible existence of standing acoustic waves (SAW) was ignored. But, in fact, from the point of view of elastic properties, our system is inhomogeneous by construction. Indeed, the difference between elasticity moduli and crystal density of GaAs and GaP could be the source of acoustic waves reflection. Moreover, due to the presence of three QW's multiple-reflection effects are expected. It follows that the GaP layers, in between the GaAs QW's, could sustain interferences of secondary reflected waves, and hence a number of standing waves.

The main physics related to coupling of SAW with electrons and their possible contribution to Raman scattering can be derived here by considering just a single GaP layer surrounded by semi-infinite GaAs layers. The atomic displacement field in both materials is obtained from the dynamical equation for the vibrational amplitude u and from the mechanical boundary conditions, i.e., the continuity of the displacement and the hydrostatic pressure at the matching interfaces [1]. This yields for longitudinal displacements in GaP

$$u \sim \cos q_z\left(z - \frac{d}{2}\right) + i\eta \sin q_z\left(z - \frac{d}{2}\right), \qquad (4)$$

in which q_z is the acoustic phonon wave vector, d (38 nm) is the GaP layer thickness, and z is the distance with respect to the center of the layer. η is related to the acoustic impedance mismatch between GaAs and GaP, i.e., $\eta = \rho_a \nu_a / \rho_p \nu_p$, where ρ_p (ρ_a) and ν_p (ν_a) are the crystal density and sound velocity in GaP (GaAs). From the bulk material parameters [17,18] we get $\eta = 0.917$. It is clear that the vibrational amplitude u given by Eq. (4) is a standing wave arising from the coherent superposition of counterpropagating plane waves.

The electron-phonon interaction Hamiltonian given by Eq. (1) must be adapted to the form of vibrational amplitude given by Eq. (4). Then, the Raman scattering efficiency associated with SAW is found to be proportional to

$$S' = \sum_{q_z} \frac{q_z^2}{\omega_{q_z}} \left[\sin^2\left(\frac{q_z d}{2}\right) + \eta^2 \cos^2\left(\frac{q_z d}{2}\right)\right] \times |M_{q_z}|^2 \delta(\hbar\omega_s - \hbar\omega_i \pm \hbar\omega_{q_z}) \,. \qquad (5)$$

In comparison with Eq. (2), some terms in Eq. (5) have been omitted for clarity. The form factor M_{q_z} is still given by Eq. (3). It follows from Eq. (5) that the standing wave character of the displacement field causes a periodic modulation of the Raman spectrum. As expected, this modulation cancels for $\eta = 1$ (i.e., for propagating plane waves).

Figure 2(a) shows an extension, in the low-frequency region, of the Raman spectrum presented in Fig. 1(b). The spectrum calculated according to Eq. (5) is also shown. The electron wave function deduced previously is used in these calculations. This means that interaction between SAW [given by Eq. (4)] and confined electrons of each QW is assumed. It is clear, from Fig. 2(a), that the observed oscillations are due to resonant Raman scattering by SAW. Frequency location, as well as amplitude, of the oscillations are well reproduced by the present model without any adjustable parameter. Moreover, from Eq. (5) one notes that intensity maxima associated with SAW occur for $q_z d = (2\ell + 1)\pi$ (ℓ is an integer number).

Figure 2(b) presents a plot of the measured oscillations frequencies versus reduced wave vector $q_z m/\pi = (2\ell + 1)m/d$, where m is the thickness of a GaP monolayer. As it can be seen, the measured frequencies perfectly fit the dispersion curve of LA phonons in (bulk) GaP.

It is worthwhile to emphasize that in the Raman spectra the SAW manifest not as additional peaks but actually as a modulation of the continuous scattering spectrum. Hence, their observation by Raman scattering requires both a strong spatial localization of electrons (nonvanishing form factor) and a rather important acoustic mismatch (high η). Basically, the SAW studied here and the folded acoustic phonon [8] associated with superlattice structures are similar in nature, as both types of excitations form coherent phonon states. However, whereas SAW arise from interference between reflected acoustic waves, folded acoustic phonons are due to coupling between Bragg-diffracted acoustic waves.

In summary, low-frequency resonant Raman GaAs QW scattering was analyzed in terms of spatial localization of electrons and their coupling to standing acoustic waves. It was shown that electron localization leads to wave vector nonconserving Raman processes, and hence to the activation of the one-dimensional density of states of acoustic phonons. This effect explains well the observed continuous emission. The strong sensitivity of this continuous emission to the details of the electronic structure has been discussed. It follows that low-frequency resonant Raman scattering can be used as an efficient probe of electronic confinement in low-dimensional structures. Moreover, the existence of standing acoustic waves in our system was established. It was found that the standing wave character is responsible for the observed oscillatory behavior of the continuous scattering. Such observations are reported here for the first time.

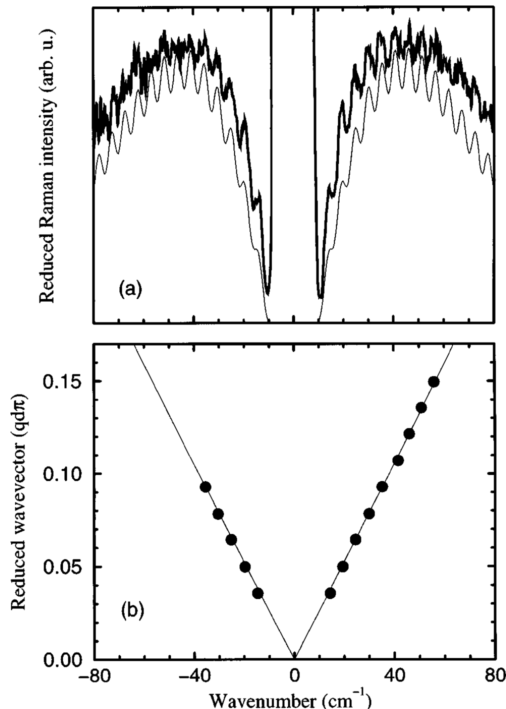

FIG. 2. (a) Low-frequency region of the spectrum presented in Fig. 1(b). The thin line shows the calculated Raman spectrum. (b) Plot of the measured oscillations frequencies (dots) versus reduced wave vector. The continuous line is the LA dispersion curve, in bulk GaP, as deduced from neutron data.

We are grateful to Professor J. P. Rino for a critical reading of the manuscript. This work was supported financially by the French/Spanish Picasso program.

[1] B. Jusserand and M. Cardona, in *Light Scattering in Solids,* Topic in Applied Physics Vol. 66 (Springer-Verlag, Berlin, 1989).
[2] E.L. Ivchenko and G. Pikus, *Superlattices and Other Heterostructures,* Springer Series in Solid State Sciences Vol. 110 (Springer-Verlag, Berlin, 1995).
[3] D.J. Mowbray, M. Cardona, and K. Ploog, Phys. Rev. B **43**, 1598 (1991).
[4] A.J. Shields, M. Cardona, and K. Eberl, Phys. Rev. Lett. **72**, 412 (1994).
[5] A. Mlayah, R. Carles, A. Sayari, R. Chtourou, F.F. Charfi, and R. Planel, Phys. Rev. B **53**, 3960 (1996).
[6] H.D. Fuchs, D.J. Mowbray, M. Cardona, S.A. Chalmers, and A.C. Gossard, Solid State Commun. **79**, 223 (1991).
[7] R. Hessmer, A. Huber, T. Egeler, M. Haines, G. Tränkle, G. Weimann, and G. Abstreiter, Phys. Rev. B **46**, 4071 (1992).
[8] C. Colvard, R. Merlin, M.V. Klein, and A.C. Grossard, Phys. Rev. Lett. **45**, 298 (1980).
[9] D. Gammon, B.V. Shanabrook, and D.S. Katzer, Phys. Rev. Lett. **67**, 1547 (1991).
[10] A. Mlayah, A. Sayari, R. Grac, A. Zwick, R. Carles, M.A. Maaref, and R. Planel, Phys. Rev. B (to be published).
[11] V.I. Belitsky, T. Ruf, J. Spitzer, and M. Cardona, Phys. Rev. B **49**, 8263 (1994).
[12] A. Fainstein, T. Ruf, M. Cardona, V.I. Belitsky, and A. Cantarero, Phys. Rev. B **51**, 7064 (1995).
[13] A. Mazuelas, L. Gonzales, F.A. Ponce, L. Tapfer, and F. Briones, J. Cryst. Growth **131**, 465 (1993).
[14] J.A. Prieto, G. Armelles, M.E. Pistol, P. Castrillo, J.P. Silveira, and F. Briones, Appl. Phys. Lett. (to be published).
[15] P.Y. Yu and M. Cardona, in *Fundamentals of Semiconductors Physics and Materials Properties* (Springer, Berlin, 1991).
[16] H. Bilz and W. Kress, *Phonons Dispersion Relations in Insulators,* Springer Series in Solid State Sciences Vol. 10 (Springer-Verlag, Berlin, 1979).
[17] S. Adachi, J. Appl. Phys. **58**, R1 (1985).
[18] O. Madelung, *Data in Science and Technology,* Semiconductors Group IV and III-V Compounds (Springer-Verlag, Berlin, 1991).